

## Supplementary Materials

# Removal of Tetracycline Hydrochloride from Water by Visible-Light Photocatalysis Using BiFeO<sub>3</sub>/BC Materials

Zhengyang Fang<sup>1,2</sup>, Honghui Jiang<sup>1</sup>, Jiamin Gong<sup>1</sup>, Hengrui Zhang<sup>1</sup>, Xi Hu<sup>1</sup>, Ke Ouyang<sup>1</sup>, Yuan Guo<sup>3</sup>, Xinjiang Hu<sup>1</sup>, Hui Wang<sup>1,4,\*</sup> and Ping Wang<sup>1,\*</sup>

<sup>1</sup> College of Environmental Science and Engineering, Central South University of Forestry and Technology, Changsha 410004, China

<sup>2</sup> Guangzhou Institute of Geochemistry, Chinese Academy of Sciences, Guangzhou 510640, China

<sup>3</sup> Institute of Bast Fiber Crops, Chinese Academy of Agricultural Sciences, Changsha 410205, China

<sup>4</sup> Faculty of Life Science and Technology, Central South University of Forestry and Technology, Changsha 410004, China

\* Correspondence: wanghui@csuft.edu.cn (H.W.); csfuwp@163.com (P.W.)

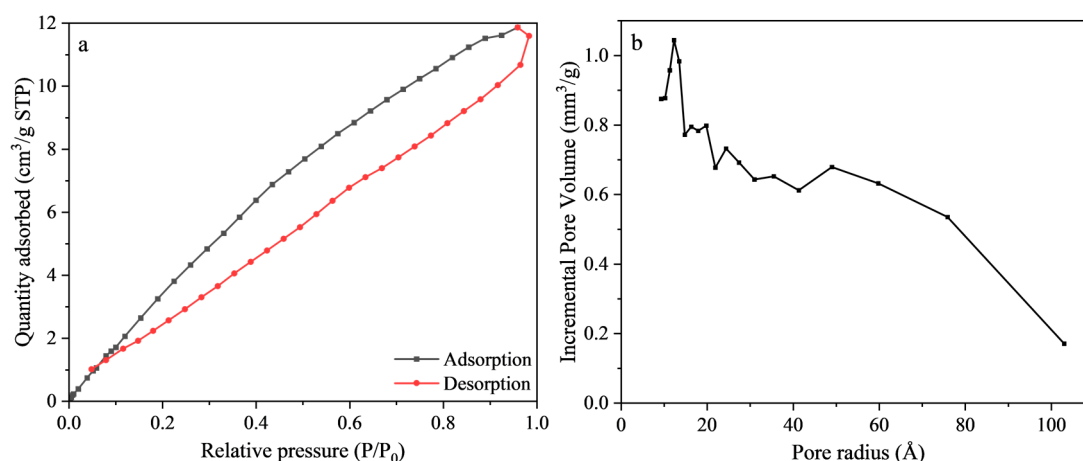


**Figure S1.** (a) Plot of N<sub>2</sub> adsorption-desorption isotherms, (b) Pore size distribution curve of BiFeO<sub>3</sub>/BC.

The N<sub>2</sub> adsorption-desorption isotherms at 77K was displayed in Figure S1a. Measured specific surface areas was 26.739 m<sup>2</sup>/g. Compared to other previous studies, BiFeO<sub>3</sub>/BC showed a larger surface area [17,56]. We speculate that the co-pyrolysis process with biomass promotes the generation of pores on the material surface. Another study also reported an increase in specific surface area due to the incorporation of biochar [57].

Figure S1b plots the pore size distribution adopting BJH adsorption method calculations. We can conclude that micropores with pore sizes between 1 and 5 nm

---

contributed the most to the specific surface area. They are the main sites where the reaction takes place and complement the catalytic performance of the material.

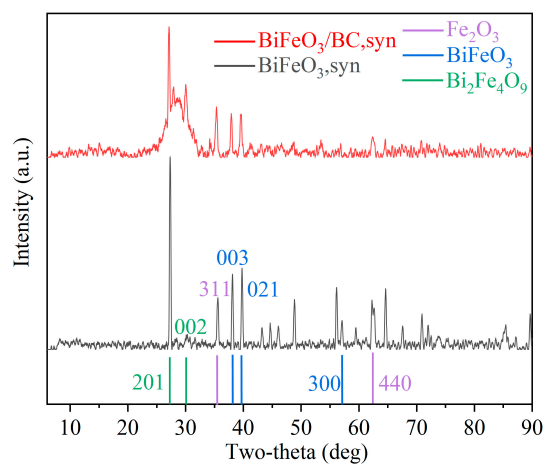


**Figure S2.** XRD patterns of  $\text{BiFeO}_3/\text{BC}$  and  $\text{BiFeO}_3$ .

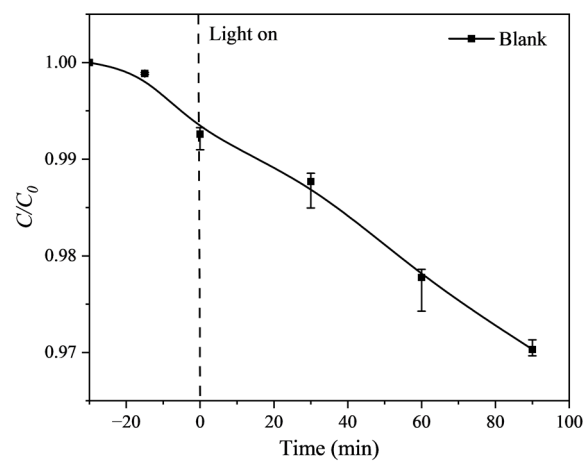


**Figure S3.** Photolysis curve of TCH (3 replicates; pH = 4;  $C_{0(\text{TCH})} = 10 \text{ mg/L}$ ).

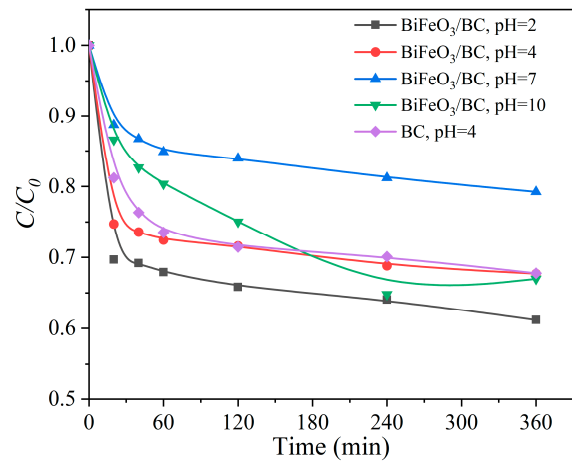


**Figure S4.** TCH adsorption by BC and BiFeO<sub>3</sub>/BC at different pH values. (Dosage of BiFeO<sub>3</sub>/BC: 0.5 g; C<sub>0(TCH)</sub> = 30 mg/L).

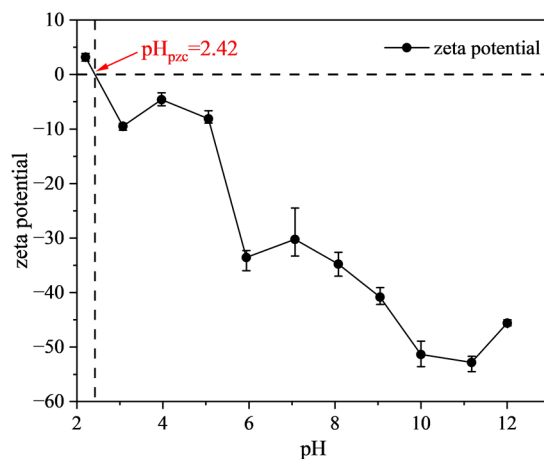


**Figure S5.** Zeta potential of BiFeO<sub>3</sub>/BC.

The results of zeta potentials of BiFeO<sub>3</sub>/BC under different pH were shown by Figure S3. The point of zero charge (pH<sub>pzc</sub>) of BiFeO<sub>3</sub>/BC material was indicated. At pH < 2.42, BiFeO<sub>3</sub>/BC was positively charged, while it became negatively charged at pH > 2.42. Meanwhile, followed by pH changes, TCH exhibited various surface charge as reported [19,58]. Therefore, at pH < 2.42, existence of repulsive force was expected between TCH cationic particles and BiFeO<sub>3</sub>/BC. Whereas at pH > 2.42, BiFeO<sub>3</sub>/BC had a negative charge on its surface and TCH was positively charged, with electrostatic attraction force working, TCH molecules were more likely to be absorbed onto BiFeO<sub>3</sub>/BC. Therefore, degradation efficiency reached highest at pH = 4.

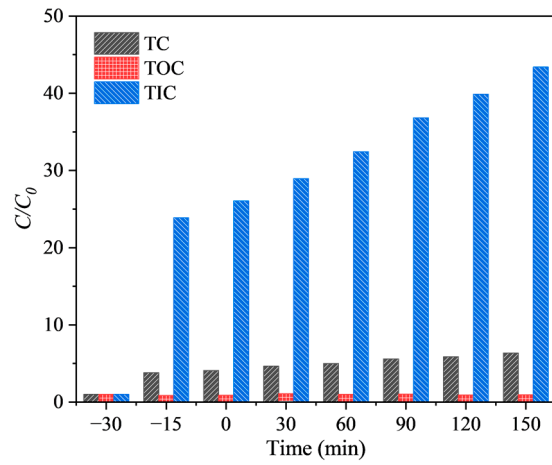


**Figure S6.** TOC photocatalytic removal efficiencies of TCH. (Dosage of  $\text{BiFeO}_3/\text{BC}$ : 0.5 g; pH = 4;  $C_{0(\text{TCH})} = 10 \text{ mg/L}$ ).

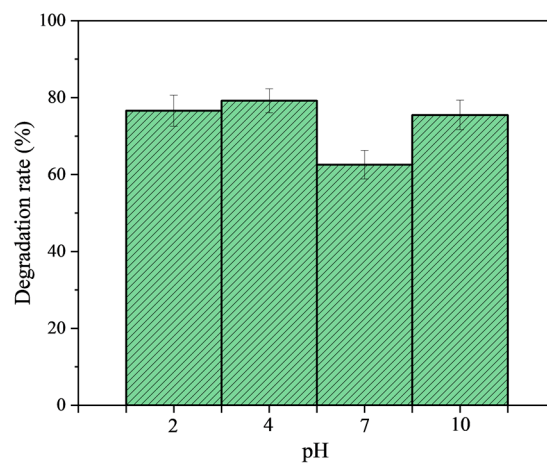


**Figure S7.** Comparison of the degradation efficiency of TCH after 90 minutes of reaction at different pH values. (3 replicates; Dosage of BiFeO<sub>3</sub>/BC: 0.5 g; C<sub>0(TCH)</sub> = 30 mg/L).

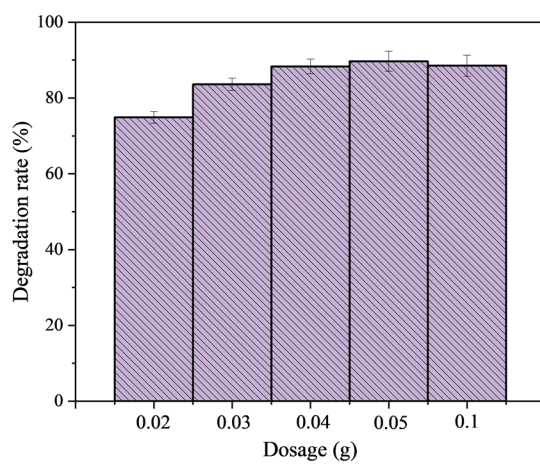


**Figure S8.** Comparison of the degradation rate of TCH after 90 minutes of reaction at different dosing rates (3 replicates; pH = 4;  $C_{0(\text{TCH})} = 10 \text{ mg/L}$ )

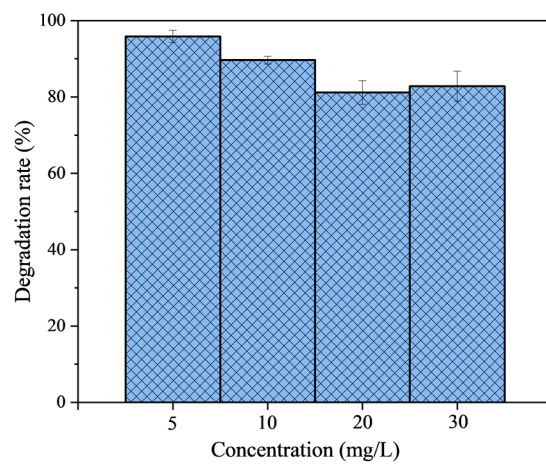


**Figure S9.** Comparison of the degradation rate of TCH after 90 min of reaction at different initial concentrations. (3 replicates; Dosage of BiFeO<sub>3</sub>/BC = 0.05 g; pH = 4).

---

## References:

56. Gao, F.; Chen, X.Y.; Yin, K.B.; Dong, S.; Ren, Z.F.; Yuan, F.; Yu, T.; Zou, Z.; Liu, J.M. Visible-light photocatalytic properties of weak magnetic BiFeO<sub>3</sub> nanoparticles. *Advanced Materials* **2007**, *19*, 2889, doi:<https://doi.org/10.1002/adma.200602377>.
57. Kumar, A.; Kumar, A.; Sharma, G.; Naushad, M.; Stadler, F.J.; Ghfar, A.A.; Dhiman, P.; Saini, R.V. Sustainable nano-hybrids of magnetic biochar supported g-C<sub>3</sub>N<sub>4</sub>/FeVO<sub>4</sub> for solar powered degradation of noxious pollutants- Synergism of adsorption, photocatalysis & photo-ozonation. *Journal of Cleaner Production* **2017**, *165*, 431-451, doi:<https://doi.org/10.1016/j.jclepro.2017.07.117>.
58. Yang, H.; Yu, H.; Wang, J.; Ning, T.; Chen, P.; Yu, J.; Di, S.; Zhu, S. Magnetic porous biochar as a renewable and highly effective adsorbent for the removal of tetracycline hydrochloride in water. *Environmental Science and Pollution Research* **2021**, *28*, 61513-61525, doi:[10.1007/s11356-021-15124-6](https://doi.org/10.1007/s11356-021-15124-6).